I&EC research
Industrial & Engineering Chemistry Research

ACS AuthorChoice

Article

pubs.acs.org/IECR


# Control of a Spinning Disc Reactor: An Experimental Study

Dena Ghiasy, Ming T. Tham,† and Kamelia V. K. Boodhoo*

School of Chemical Engineering and Advanced Materials, Newcastle University, Newcastle upon Tyne, NE1 7RU United Kingdom

**ABSTRACT:** Despite abundant experimental work on intensification aspects of spinning disc reactors (SDRs), research on control characteristics of such novel devices are rather scarce. Control of SDRs may be challenging due to fast dynamics and high responsiveness of the system. However, the readily controllable rotational speed of the disc may offer an extra degree of freedom in control system design. In the present work, two test processes, namely, neutralization of HCl and NaOH and precipitation of barium sulfate, are chosen to investigate the control aspects of SDRs experimentally. The most commonly used controllers based on PI/PID algorithms implemented in LabVIEW, coupled with commercially available instrumentation, are employed to achieve the control objectives. The pH control of the neutralization process was successfully achieved using a PID controller which manipulated the flow rate of the base stream to the SDR. Addition of a disturbance observer scheme resulted in further enhancement of the control performance by suppressing the undesired effects of pH system nonlinearity. The conductivity control of the precipitation process was successfully achieved by manipulating the disc rotational speed, which presents a vastly appealing potential for adopting an innovative approach to process control for SDRs.

## 1. INTRODUCTION

The spinning disc reactor (SDR) is a classic example of process intensification with various attractive features such as enhanced heat/mass transfer capabilities and the ability to handle viscous liquids.[1,2] Although abundant experimental work is available in the literature on intensification aspects of SDRs,[3−7] very little has been done on devising appropriate control strategies for the unit. Effective control of SDRs may be challenging due to their fast dynamics and short residence times, as discussed in an earlier publication.[8] However, some key features of SDRs may prove to be advantageous from a control point of view. For example, the rotational speed of the disc offers an extra degree of freedom in control system design. The residence time and mixing intensity, which directly influence parameters such as conversion and particle size, may be controlled by adjusting the disc rotational velocity as well as the more commonly used methods of varying reactant flow rates. Lim[9] and Aoune and Ramshaw[10] studied the gas−liquid mass transfer performance of SDRs for absorption of $O_2$ into thin liquid films. Their results implied a strong link between the disc rotational speed and achieved mass transfer coefficient. More recently, Burns and Jachuck[11] studied the precipitation of $CaCO_3$ on a spinning disc reactor and found that conversion was affected by both feed flow rate and disc rotational speed. Cafiero et al.[12] also showed that $BaSO_4$ crystal production rate increases with increasing rotational speed while the average crystal size decreases.

In the present study, the control aspects of SDRs are studied experimentally for two example processes. The first process involves pH control in a strong acid/strong base neutralization reaction, wherein the effluent pH is controlled by manipulating the base stream flow rate. The second process is a precipitation reaction where the conductivity of the effluent stream is controlled by manipulating the disc rotational speed. Intensified equipment may not be considered commercially viable if sophisticated and complex control schemes, which require significant expertise to implement, are needed to achieve satisfactory control performance.[8] For this reason, in the present study, the control objectives are achieved by the most commonly used PI/PID controllers, coupled with commercially available instrumentation, with a view to highlight any potential challenges/limitations that may prevail in the application of such conventional controllers and instrumentation to the SDR technology.

## 2. THEORETICAL BACKGROUND

**2.1. pH Control.** SDRs are particularly suited for inherently fast chemical reactions whose rates are often impeded in conventional reactor systems due to mass transfer limitations. Neutralization reactions are intrinsically fast, and provided the mixing limitations can be overcome, the reaction can be completed within the short residence times of SDRs. pH control is often a challenging task due to both the nonlinear and time-varying characteristics of the system, particularly for strong acid/strong base neutralization processes. Thus, control strategies which are both nonlinear and adaptive may be required to achieve satisfactory control performance by accounting for the nonlinearity and time-varying characteristics of pH systems, respectively.[13] However, as previously indicated, the objective of the present work is to assess the controllability of SDRs using conventional PID controllers along with commercially available sensors and actuators.

Nonadaptive linear controllers such as those based on a PID algorithm are the simplest strategy for pH control, which operate on one set of tuning parameters. In a pH system, the process gain is determined by the slope of the titration curve which varies significantly for the case of strong acid/base systems, as shown in Figure 1. The required controller gain is usually inversely proportional to the process gain; therefore, at

**Received:** June 26, 2013
**Revised:** October 10, 2013
**Accepted:** October 31, 2013
**Published:** October 31, 2013

  

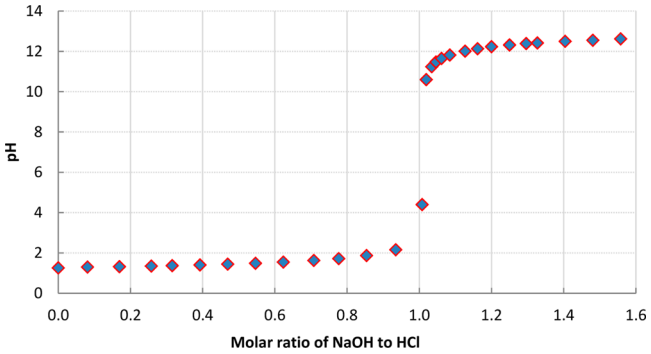


**Figure 1.** Titration curve.

steep regions of the titration curve (near the equivalence point) where the process gain is high, the controller gain should be set low to maintain stability. Conversely, at flat regions of the titration curve (acidic and basic regions) where the process gain is low, the controller gain may be set higher to achieve a faster response without approaching the stability margins. Theoretically, a nonadaptive linear PID controller provides adequate performance only if the process is operated within a narrow region where the controller is tuned for and if the buffering variations are small.[14]

Occurrence of limit cycles (uniform oscillations with fixed magnitude) in a pH control loop is a common problem[15] due to highly nonlinear dynamics of the neutralization processes. Figure 1 shows the tremendous sensitivity of the system between pH 2 and 12 where the titration curve has the steepest slope. Within this range, the process gain is very high implying that small variations in the reagent flow leads to significant changes in the effluent pH, giving rise to the occurrence of limit cycles.

As mentioned previously, it is of particular interest to assess the possibility of using the disc rotational speed to achieve a control objective. Although neutralization reactions have very fast kinetics and are generally considered to be mixing limited, adjusting the rotational speed in the present work did not lead to significant changes in the effluent pH. This observed lack of sensitivity may be attributed to adequate mixing having already been achieved at the lowest disc speed of 200 rpm for the set of concentration and flow rates examined. Therefore, increasing the rotational speed further, which results in even better mixing, does not influence the rate of reaction nor the pH of the effluent stream under the chosen operating conditions. Although different sets of flow rates and concentrations may give rise to different levels of sensitivity of the effluent pH to rotational speed, we chose instead to use flow rate as the manipulated variable for the pH control in the SDR and we implemented a different process which showed a more readily detectable sensitivity to rotational speed, as outlined next.

**2.2. Barium Sulfate Precipitation.** Most crystallization reactions have fast kinetics, implying that the rate of reaction can be influenced by how effectively the reactants are mixed on the molecular scale. In the present work, reactive crystallization of barium sulfate is selected as an example process to study the potential of exploiting the rotational speed of SDRs as a manipulated variable to achieve a given control task. Our selection of this particular process is based on evidence in the literature that the rate of $BaSO_4$ precipitation formed from mixing barium chloride and sodium sulfate in a SDR is a function of the disc rotational speed.[12] This precipitation proceeds according to eq 1:

$$BaCl_2\,(aq) + Na_2SO_4\,(aq) \rightarrow BaSO_4\,(s)\downarrow + 2NaCl\,(aq) \quad (1)$$

Barium sulfate is sparingly soluble in water and therefore precipitates as soon as it is formed. A number of processes occur almost simultaneously during such precipitation reactions, including mixing of the reactants, chemical reaction, nucleation, and growth of the solid particles. Secondary processes such as agglomeration, ripening, and breakage may also occur. The mechanism and kinetics of nucleation and growth are mainly controlled by the degree of supersaturation.[16]

High supersaturation levels, generated by enhanced mixing, is as necessary as control and prevention of particle agglomeration to achieve nanosized precipitated crystals[17] which are desirable from the point of view of their superior properties such as enhanced dissolution rates in pharmaceutical applications.[18] Therefore, intensified reactors such as SDRs and micro/millireactors offer great potentials for production of nanoparticles with tight distributions as they are able to provide high levels of uniform micromixing[2,19] to enhance the nucleation rate throughout the reaction volume. These technologies also offer extremely short and controllable residence times to limit particle growth and/or agglomeration. Their hydrodynamic characteristics are readily controlled by adjusting the liquid flow rate, channel diameter in micro/millichannel reactors, and rotational speed in SDRs. These offer extra degrees of freedom and more flexibility in controlling the precipitation process, including the crystal size and morphology, as shown by Cafiero et al.[12] and by McCarthy et al.[20] who produced $BaSO_4$ particles in a SDR and in a millimeter scale channel reactor, respectively.

Of particular relevance to the present study, Cafiero et al. found that the crystal production rate increased while the average crystal size decreased with increasing rotational speed.[12] This behavior was attributed to an increase in the micromixing intensity within the thin liquid film traveling across the disc at higher disc speed, a fact which has been independently verified in micromixing studies in the SDR.[21] Micromixing not only affects nucleation rate mainly by controlling the generation and distribution of supersaturation but also influences the kinetics of crystal growth by influencing mass transfer and diffusion.[22] If mixing limitations are overcome, the overall rate of consumption of reacting ions via nucleation and growth is determined by the kinetics of these processes. Thus, the impact of residence time on extent of reaction can become important if one of these processes is quite slow. Crystal growth tends to be slower than homogeneous nucleation and is therefore the rate controlling step for ion consumption. Also, over the course of a precipitation process, the thermodynamic supersaturation level decreases with time as the ions are consumed. Typically, when supersaturation has decreased to a low level after a relatively long residence time in a crystallizer, crystal growth becomes dominant, and therefore, larger crystals are produced. Conversely, at high supersaturation levels (i.e., at the start of the process when the reagents have been in the crystallizer for a short residence time), the nucleation rate is much faster than the linear growth rate and therefore finer particles are produced.[23] The increased particle size with increasing residence time in continuous precipitation of barium sulfate is


dx.doi.org/10.1021/ie4020149 | Ind. Eng. Chem. Res. 2013, 52, 16832−16841

also evident in the experimental data presented by Pohorecki and Baldyga.[24]

The challenges involved in the control of precipitation/crystallization processes are summarized by Braatz[25] to be due to significant uncertainties in the kinetics, the ambiguity in effects of mixing, process nonlinearity, and sensor limitations. For effective identification and control of a precipitation process, measurements of the solution concentration and crystal size distribution are required. Attenuated total reflection-Fourier transform infrared (ATR-FTIR) and Raman spectroscopy have been used to measure the solution concentration for feedback control of crystallization processes.[26,27] Devices based on the laser backscattering approach may be used to provide in situ measurement of the particle size and distribution.[28] However, in most industrial crystallization processes, only easily measurable parameters such as temperature, flow rate, level, and pressure are used to control the process, while online measurements of particle size and solution concentration are seldom used as feedback signals in the control loop.[29]

During any precipitation reaction, the solution conductivity is reduced as the reacting ions precipitate out and no longer contribute to the solution's conductivity. For very dilute solutions of a strong electrolyte (one that freely dissociates), conductivity increases linearly with increasing concentration of ions. The conductivity−concentration relationship becomes progressively nonlinear as the ion concentrations in the solution increase, due to increased level of ion interactions. In very concentrated solutions, the attractive forces between charged ions can give rise to ion association and formation of neutral particles; thus, conductivity begins to fall.[30] Taguchi et al.[31] used conductivity measurements to calculate the thermodynamic supersaturation in a series of barium sulfate batch precipitation reactions. The calculated supersaturation profiles showed measurable sensitivity to the stirrer speed, wherein the rate of decay of supersaturation was faster at higher rotational speeds. Stanley[32] also used conductivity measurements to monitor concentration variations in semibatch precipitations of barium sulfate. The results indicated sensitivity of the conductivity profile to stirrer speed, where faster reaction rates prevailed at higher agitation intensities. The same trend is also reported by Rodgers et al.[33] for precipitation of barium sulfate in a semibatch stirred vessel. The main drawback of using conductivity measurements to infer concentrations of reacting ions is that other nonreacting ions and impurities can also influence the conductivity readings and therefore deteriorate the control performance. Further, the correlation between conductivity measurements and supersaturation may be time-varying as a result of process disturbances. Therefore, the application of conductivity measurements for control of an industrial precipitation process may not be straightforward. However, for the purpose of the current research in a controlled lab environment, using conductivity measurements for feedback control of the precipitation process is deemed to be the simplest and most attractive approach.

## 3. EXPERIMENTAL SET UP AND PROCEDURES

The control algorithms for the two aforementioned processes are implemented in National Instrument's LabVIEW software.[34] The feedback control loops for the pH control and conductivity control in barium sulfate precipitation are illustrated in Figures 2 and 3, respectively.

For the pH control experiments, 0.1 M solutions of the acid and base are pumped on to the center of the SDR while the

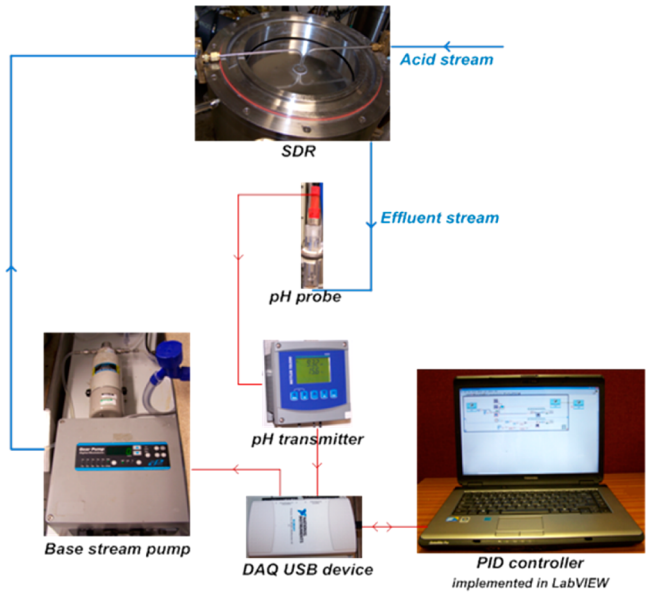


**Figure 2.** Feedback control loop (pH control).

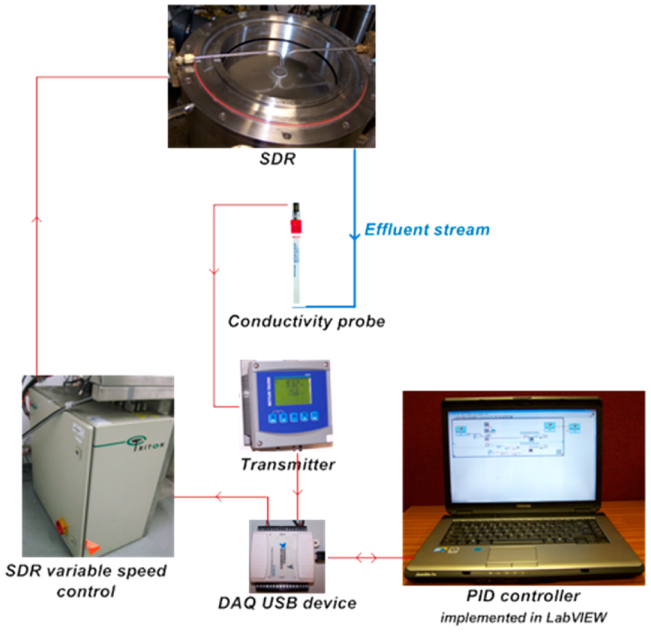


**Figure 3.** Feedback control loop (conductivity control).

disc temperature and rotational speed are maintained at set values (25 °C and 750 rpm). The SDR consists of a horizontally mounted smooth disc of 16 cm diameter. The pH of the effluent stream is measured by a Mettler-Toledo InPro 3253i/SG/120 pH probe, and a corresponding signal is transmitted to a PC via a Mettler-Toledo M300 transmitter and a National Instrument data acquisition device (NI-USB6211). The PID controller which is implemented in LabVIEW 2009 SP1 compares this signal with the desired value or the set point and computes an appropriate response (eq 2) which is fed back to the data acquisition device and subsequently to the actuator, the base stream variable speed pump in this particular case, where the controller's command is implemented.

$$c(t) = K_c\left(e + \frac{1}{T_i}\int_0^t e\,dt + T_d\frac{de}{dt}\right) \quad (2)$$


dx.doi.org/10.1021/ie4020149 | Ind. Eng. Chem. Res. 2013, 52, 16832−16841

This feedback control loop (as depicted in Figure 2) is executed continuously in order to maintain the effluent pH at a desired value. A similar control loop set up is employed for the effluent conductivity control in the precipitation process. The main difference is that the PID controller's command is sent to the SDR variable speed drive unit which manipulates the disc speed, as illustrated in Figure 3. The conductivity of the effluent stream is measured using a 4 pole Mettler-Toledo InPro7100i sensor. Solutions (0.01 M) of barium chloride and sodium sulfate (made up using deionized water) are pumped on to the center of the disc at flow rates of 5 mL/s each. The conductivity signal was initially acquired by the same data acquisition device used for the pH control (NI-USB6211). However, there were often large amplitude spikes in the measured signal. A less sensitive device (NI-USB6008) was used instead to eliminate the spikes although measurement noise of about 5 $\mu$S/cm was still present in the signal. The simplest way to reduce the degree of variation in the signal is to add a filter to the acquired data. In the present study, a first order filter was implemented in LabVIEW on the path of the incoming conductivity signal. Increasing the filter time constant will enhance the noise reduction capability of the filter but at the expense of larger measurement lags. Improved filter design and perhaps hardware filter considerations were outside the scope of the current work.

Since this control setup involves both hardware and software operations, it is critical to ensure that the software and hardware operations are adequately synchronized. For the pH control case, the rate of loop execution (period) was selected as 100 ms and the loop was executed once for each sample point acquired. However, since a different data acquisition device was used for the conductivity control, the sampling rate and loop period had to be adjusted (2 Hz and 500 ms) to meet the capability of the closed loop execution speed.

The controllers were fine-tuned manually using initial control parameters obtained by applying the Direct Synthesis Method[35] to a first order process model generated via input−output tests. For the pH control system, a PID controller with a gain of 0.025 and integral and derivative time constants of 0.43 and 0.11 min was used. However, since conductivity signal to the controller for the barium sulfate precipitation process was rather noisy, the derivative term was not used and a PI controller with a gain of −10 and an integral time constant of 0.3 min was employed.

The control performance in terms of set point tracking is assessed for both processes, while the disturbance rejection capability of the PID controller is also investigated for the neutralization process. The disturbance was implemented by varying the flow rate of the influent (acid) stream.

## 4. RESULTS AND DISCUSSION

### 4.1. pH Control of HCl/NaOH Neutralization Process.

At steady state, the flow rate of the influent (acid) stream is equal to 5 mL/s. To assess the disturbance rejection capability of the PID controller, the influent flow rate was first increased by 20% and then returned to the baseline before a 20% reduction was applied. The disturbance rejection performance of the PID controller is presented in Figure 4. It can be seen that the controller is able to recover from the imposed disturbances and the process variable (effluent pH) is brought back to the set point. However, the process variable oscillates around the set point value, with the largest oscillations occurring when the acid flow is reduced by 20% from the steady state value.

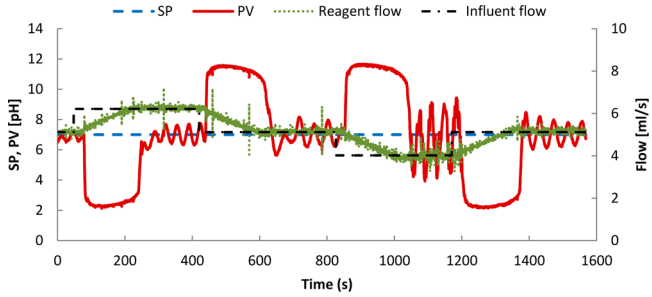


**Figure 4.** PID controller disturbance rejection performance [SP: set point, PV: process variable (effluent pH)].

The constant oscillations or limit cycles are a common problem in pH control, particularly near the equivalence point for strong acid/strong base systems. Although the controller gain is set to a small value (0.025) implying that the corrective action is very small, the heightened sensitivity of the system to reagent addition between pH 2 and 12 causes the process variable to oscillate around the set point. The small value of the controller gain also implies that, at acidic and basic regions where the slope of the titration curve is low, the controller performance will be sluggish, as observed in Figure 4.

From a control perspective, the disturbance rejection performance is rather poor due to the sluggish response and the presence of limit cycles. However, this outcome is not unexpected when a linear controller is applied to a highly nonlinear control task; the tuning parameters obtained at the nominal operating point result in inadequate performances in different operating regions. Nevertheless, the results indicate that the notoriously difficult task of pH control can still be achieved in a SDR using a PID controller coupled with commercially available instrumentation, despite the fast dynamics of the SDR.

Disturbance observer (DO) design is a complementary algorithm which is effective in estimating and canceling out the unmeasured disturbances. The DO algorithm was employed by Shahruz et al.[36,37] to suppress the undesired effects of system nonlinearity in control of backlash in gear systems. The results indicated that DO structures are effective means of suppressing limit cycles. The application of the DO to a pH control problem in a SDR was investigated in previous research via simulation[8] and its online implementation is investigated in the present work. The nominal plant model used in the DO algorithm is determined by input−output tests,[8] and the filter time constant is selected as 180 s. Addition of the DO scheme leads to considerable improvement of the disturbance rejection performance (Figure 5) where the occurrence of limit cycles is

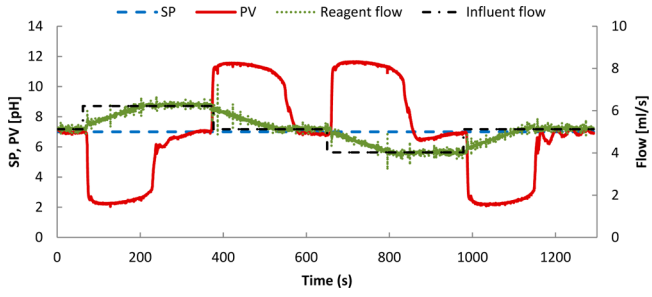


**Figure 5.** PID controller plus DO disturbance rejection performance [SP: set point, PV: process variable (effluent pH)].


dx.doi.org/10.1021/ie4020149 | Ind. Eng. Chem. Res. 2013, 52, 16832−16841

significantly suppressed. However, a more sluggish response is also observed compared to the PID scheme. Since inclusion of the DO scheme reduces the undesired effects of the system nonlinearity, larger controller gains may be used to achieve faster responses without approaching the stability margins of the system. In the present work, the same controller tuning parameters are used for both schemes to provide a benchmark for comparison and investigation of the impact of including the DO scheme, independent of the influence of controller tuning parameters. Thus, further enhancement of the performance of the PID plus DO scheme by fine-tuning the controller is not considered here.

The reproducibility of the pH control runs in our study was satisfactory. The variability in the controlled process variable (pH) was generally less than 1% as shown in Figure 6,

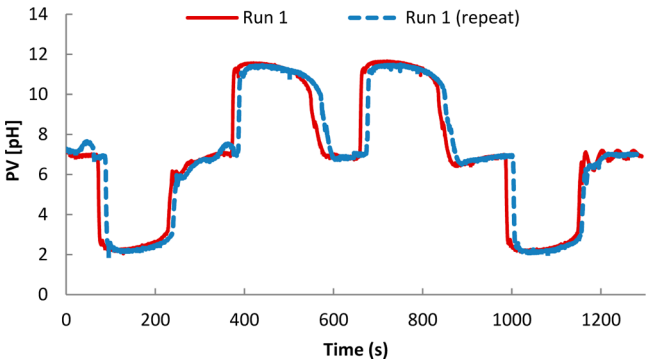


**Figure 6.** Assessment of repeatability in pH control runs.

especially in the high and low pH ranges. Because the pH control of a strong acid/strong base system around the neutral point is extremely sensitive, minor variations in the experimental conditions, such as the changes in the feed concentration from batch to batch, would have noticeable impacts on the control outcome. This may explain the more visible differences in the profiles at time periods between 350 and 400 s and again beyond 1200 s at close to pH 7.

The set point tracking performance of the PID controller is also quite acceptable as presented in Figure 7. Again, the

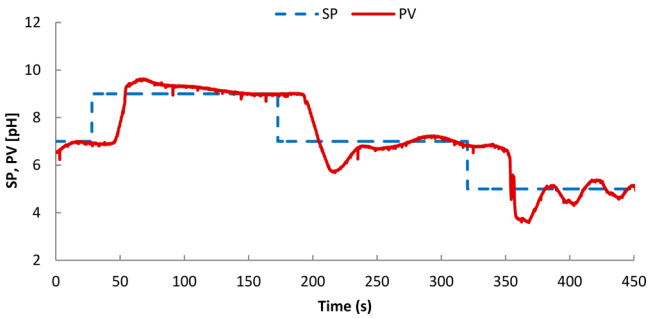


**Figure 7.** PID controller set point tracking performance [SP: set point, PV: process variable (effluent pH)].

control performance is sluggish in some operating regions while oscillations are present in other regions, due to application of a linear controller to a nonlinear control task. The large lags evident in the process response are mainly attributed to the pure time delay introduced in the current setup by the pH probe positioning downstream of the SDR and also to the slow response of the probe. This method of monitoring the process variable includes some undesired "tail effects" which may not be associated with the SDR itself. One way to overcome the problems associated with such time delays in the current setup would be to implement predictive control algorithms, the most basic being the Smith Predictor.[35] However, this was not attempted in the present study because our intention was simply to investigate whether the PID controller, an industry standard, would be capable of achieving the desired control objectives. In an ideal SDR setup, the process dynamics in the film on the disc surface would be isolated from the undesired end effects by designing and incorporating sensors with adequately fast response times within the disc itself. In this way, more effective control based on the real time measurements of the process variable on the disc could be achieved. One such approach has been demonstrated by Burns and Jachuck[11] who reported obtaining real-time measurements of the liquid film conductivity using concentric electrodes embedded on the disc at selected radial intervals.

**4.2. Conductivity Control of Barium Sulfate Precipitation Process.** The set point tracking performance of the PI controller in maintaining the conductivity of the effluent stream at the desired set point by adjusting the disc rotational speed is presented in Figure 8. The results are immensely encouraging as they show that the disc rotational speed can successfully be used as a manipulated variable to achieve a given control task in a SDR. These findings present a vastly appealing potential for adopting an innovative approach to process control for SDRs and other similar intensified technologies which offer extra degrees of freedom in design. From a strictly control point of view, the set point tracking performance could still be improved by first improving the signal conditioning of the incoming signal and second by devoting more effort to fine-tuning the controller. This, however, is not the focus of the present study which is mainly aimed at exploring the possibility of using the rotational speed as the manipulated variable as opposed to the conventional methods of flow rate and/or temperature manipulation to achieve the conductivity control objective.

Figure 9 presents the average conductivity data at various rotational speeds extracted from the closed-loop run presented in Figure 8. The standard deviation in these measurements was estimated from repeat runs under identical conditions to be about 3% which may be attributed to a combination of two factors. First, a variability of 1% in the concentrations of any one of the ionic solutions could account for a deviation of about 1% in the conductivity of the system. Second, and more importantly in our view, the profound sensitivity of the measurements to the build-up of precipitates on the disc and the probe was readily observable in our investigation. The particle build up on the probe impairs the accuracy of the conductivity measurements over time leading to time varying characteristics, as well as large measurement delays. Such accumulation of material on the disc can also arguably alter the course of precipitation, by inducing secondary nucleation, for example. This problem is more severe at high concentrations, which is the reason we limited our study to solution concentrations of 0.01 M.

It can be noted from Figure 9 that the conductivity, which is representative of the conversion, is more sensitive to the rotational speed up to disc speeds of approximately 800 rpm, beyond which disc speed appears to have no influence. This is also readily observable in Figure 8 toward the end of the run, where the controller increased the disc rotational speed from around 800 to 1300 rpm in the failed attempt to bring the

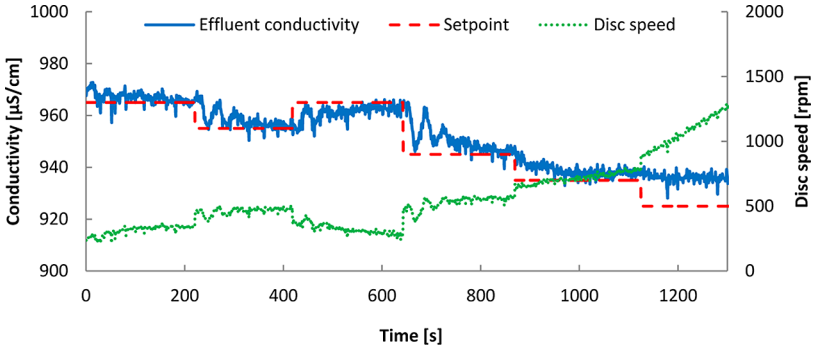


**Figure 8.** Set point tracking of conductivity by disc speed adjustment.

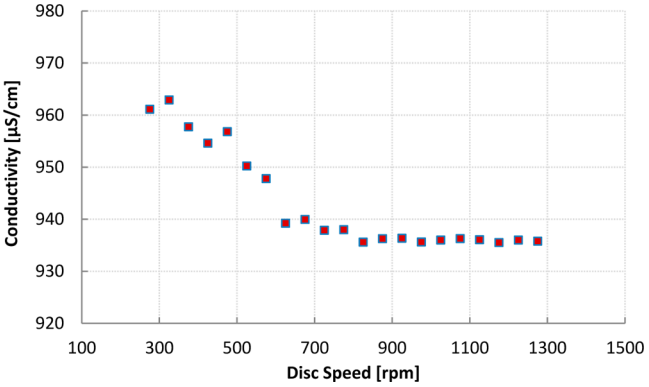


**Figure 9.** Conductivity versus disc rotational speed.

process variable to the set point, following the final step change. These findings are in good agreement with the results reported by Cafiero et al.[12] whereby the crystal production rate increased with a rise in the rotational speed up to a certain point beyond which no significant changes were observed. This phenomenon is considered as a system constraint in terms of controller design, where the process variable is nonresponsive to the controller's command. It may be explained by considering the opposing effects of increased disc speed on mixing and residence time. As the rotational speed is increased, the liquid residence time on the disc is reduced. Therefore, conversion should steadily decline (or conductivity should rise) with increasing rotational speed if the reaction is kinetically limited. However, if the reaction is mixing limited, conversion should increase with increasing rotational speed due to enhanced mixing in thinner, more intensely mixed films, according to the developed expressions for the film thickness[5] in eq 3.:

$$\delta = \left(\frac{3Q\nu}{2\pi\omega^2 r^2}\right)^{1/3} \tag{3}$$

An optimum rotational speed or range of rotational speeds may therefore exist which provides a balance between good mixing and sufficient residence time to give the highest yield. A trade-off rotational speed has indeed been observed in previous experimental studies in the SDR where conversion and selectivity were of particular interest.[4,7] It is also worth noting that similar opposing effects between mixing and residence time may also prevail by adjusting the feed flow rates in the SDR.[38] Therefore, regardless of whether the disc rotational speed or the feed flow rate is used to control a reaction, the cutoff points where enhanced mixing is counter-balanced by reduced residence time needs to be defined, where applicable. These characteristics of SDRs give rise to the postulation that perhaps advanced control algorithms are required to account for such complex interactions of the film hydrodynamics with the manipulated variables, particularly in the presence of process disturbances.

In the present study of the precipitation process, however, the profile in Figure 9 seems to suggest that the process is mixing limited between disc speeds of 200 and 800 rpm, but beyond 800 rpm, the reduced residence time has no major impact on the process yield. To better understand these effects for this particular process, an analysis of the mixing and reaction kinetics in terms of their respective time scales is useful.

*4.2.1. Effect of Mixing.* Micromixing is an important consideration in fast chemical reactions such as precipitation processes. For micromixing to have a significant effect on the course of any reaction, the micromixing time must be comparable or larger than the reaction time.[39] It is therefore useful to compare the theoretical micromixing times obtained on the disc under the different hydrodynamic conditions employed in this study with the induction time of the barium sulfate precipitation process, following a similar approach adopted by Cafiero et al.[12]

Baldyga et al.[16] developed the following expression for calculation of the micromixing time constant for molecular diffusion accelerated by deformation:

$$\tau_{micro} \cong 2\left(\frac{\nu}{\varepsilon}\right)^{0.5} \operatorname{arcsinh}(0.05Sc) \tag{4}$$

For Schmidt numbers smaller than 4000, the micromixing time constant by engulfment may be approximated as:[16]

$$\tau_{micro} \cong 17.3\left(\frac{\nu}{\varepsilon}\right)^{0.5} \tag{5}$$

The kinematic viscosity of water at 25 °C is $8.9 \times 10^{-7}$ m$^2$/s, while the diffusion coefficient of barium sulfate in water using the Scheibel equation is estimated to be $1.49 \times 10^{-9}$ m$^2$/s.[40] Thus, the resulting Schmidt number for the present system is equal to 597, implying that the micromixing in this study is more closely represented by engulfment. Therefore, eq 4 should be used to calculate the micromixing time constant, which is a more conservative value than that predicted by eq 4 (about 2× higher). A recent study into micromixing time and its effects on barium sulfate nucleation in a SDR further reinforces the use of eq 5 over eq 4.[41]

The energy dissipation rate may be estimated using the following theoretical expression[12] which has been derived from experimentally validated theoretical considerations established earlier by Khan:[42]


dx.doi.org/10.1021/ie4020149 | Ind. Eng. Chem. Res. 2013, 52, 16832−16841

$$\varepsilon = \frac{1}{2t_{res}}[(r^2\omega^2 + u^2)_o - (r^2\omega^2 + u^2)_i] \quad (6)$$

where the fluid residence time and radial velocity on a rotating surface is determined from eqs 7 and 8 respectively:[5,10]

$$t_{res} = \left(\frac{81\pi^2\nu}{16\omega^2Q^2}\right)^{1/3}(r_o^{4/3} - r_i^{4/3}) \quad (7)$$

$$u = \left(\frac{Q^2\omega^2}{12\pi^2 r\nu}\right)^{1/3} \quad (8)$$

Note that eqs 7 and 8 (as well as eq 3 for film thickness above) are based on the Nusselt treatment for smooth, laminar films derived on the basis of a simple force balance on the film in the radial direction.[5] The Nusselt profiles have been shown to be generally applicable beyond a so-called "spin-up" radius up until which the fluid initially accelerates on the disc. Using the empirical model developed by Burns and Jachuck,[11] we have estimated the spin-up radius for the conditions used in our study to be in the range of 3.9 cm (at 1600 rpm) to 5.2 cm (at 200 rpm), implying that the spin-up zone occupies no more than about 40% of the inner surface area of the disc under all disc operating conditions employed. Therefore, a minimum Ekman number (defined by eq 9) of 2.5 ensures that the Nusselt flow analysis is valid for all disc speeds in our study. This minimum value compares reasonably well with the corresponding value of 1.6 determined by de Caprariis et al.[43] on the basis of CFD analysis of film flow on the disc.

$$Ek = \left(\frac{2\pi}{3}\right)^{2/3}\left(\frac{r^4\omega\nu}{Q^2}\right)^{1/3} \quad (9)$$

As presented in Figure 10, the micromixing time constants for a total flow rate of 10 mL/s and rotational speeds of 200–1600 rpm, range from 8.3 to 0.4 ms, respectively. In comparison to these micromixing times, the induction time of 13.02 ms for the experimental conditions adopted here is larger (Table 1). The highest micromixing time is nevertheless of the same order as the induction time which could explain why the process shows some mixing limitations characteristics in the lower disc speed range, as highlighted by the drop in conductivity between 200 and 800 rpm in Figure 9. However, at the very high speeds, there is an order of magnitude reduction in the micromixing time which would make the reaction much less sensitive to mixing conditions. It is to be noted that, as the feed concentration is increased, the induction time is reduced as seen in Table 1, and thus, it is expected that micromixing would then become the controlling mechanism over a wider range of disc speeds. This has indeed been experimentally verified by Cafiero et al.[12] who found that, at a supersaturation ratio of 2000, the enhancement in micromixing at the higher disc speed of 1000 rpm further improved the number of particles formed. In this present study though, we could not carry out extensive control studies at concentrations higher than 0.01 M because of unreliable and fluctuating data due to excessive precipitation and crystal build-up over time both on the stainless steel disc and the conductivity probe at these elevated concentrations. Oxley et al.[3] reported a similar problem with a stainless steel disc where the problem was overcome by coating the disc with a thin layer of PTFE. While such an approach could be implemented in this work, the problem with the coating of the probe downstream would still need to be addressed. Until a better online measurement system that can avoid crystal build-up can be devised, limitations of usable concentration range in such control studies are likely to remain.

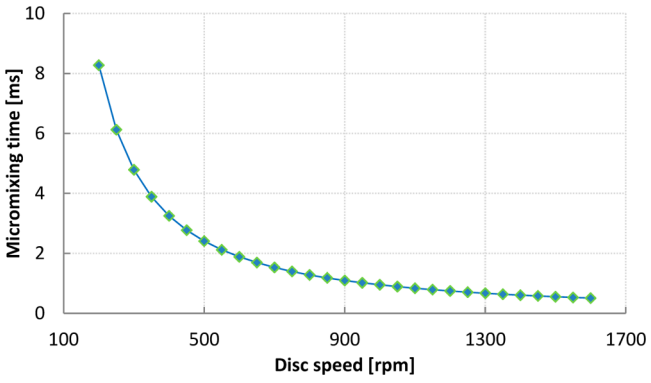


**Figure 10.** Influence of disc speed on micromixing time constant.

**Table 1. Induction Times for Different Reagent Concentrations**

| $C_{feed}$ [M] | $\gamma^a$ | $S^b$ | induction time$^c$ [ms] |
|---|---|---|---|
| 0.01 | 0.4068 | 388 | 13.02 |
| 0.1 | 0.15 | 1430 | 2.28 |
| 1 | 0.0389 | 3709 | 1.04 |

[a]Estimated from Bromley's method.[44] [b]Calculated from McCarthy et al.[20] [c]Estimated from Cafiero et al.[12]

*4.2.2. Effect of Residence Time.* The theoretical fluid residence times on the disc surface are estimated from eq 7 to be between 0.35 s at 200 rpm and just under 0.1 s at 1600 rpm at a fixed flow rate $Q$ of 10 mL/s and fluid kinematic viscosity $\nu$ of $10^{-6}m^2/s$. Noting that the conductivity probe is situated downstream of the SDR, the overall fluid residence time within the system before a measurement is made at the probe location would be longer than the values calculated because of the transport lags. A minimum of 5 s additional residence time downstream of the disc should be accounted for, during which further conversion may occur, albeit in a less intense mixing regime. In the current setup of our SDR, it is thus expected that nucleation mostly occurs while the fluid is on the disc as this is where intense micromixing prevails and therefore where local supersaturation is at its highest levels. The more nucleation sites there are (i.e., at higher micromixing), the higher the conversion is expected to be, until a fixed number of nuclei can possibly be formed. Downstream of the SDR, ions will most likely be consumed during the crystal growth process governed by diffusion. It should be pointed out that in our work we do not expect aggregation to play a major part in the precipitation process as our nucleation rates are not expected to be as high and therefore nuclei are unlikely to be as small as have been shown to be necessary for aggregation to be considered as important as the growth process.[45]

The residence time can have a potential limiting impact on the extent of reaction or conversion only if it is smaller than the overall reaction time for ion consumption, which includes nucleation time (likely to be short) and a longer crystal growth time. A theoretical analysis of the reaction time characteristics of the barium sulfate precipitation process (which includes reaction, nucleation, and crystal growth) has been developed by

Öncül et al.[46] on the basis of direct solution of the barium sulfate moment equations, which predicts the concentration profiles of the chemical species within a homogeneous reaction zone with respect to time. The semianalytical model has been used to predict the concentration profiles expected in this work (Figure 11) using the previously determined activity coefficient

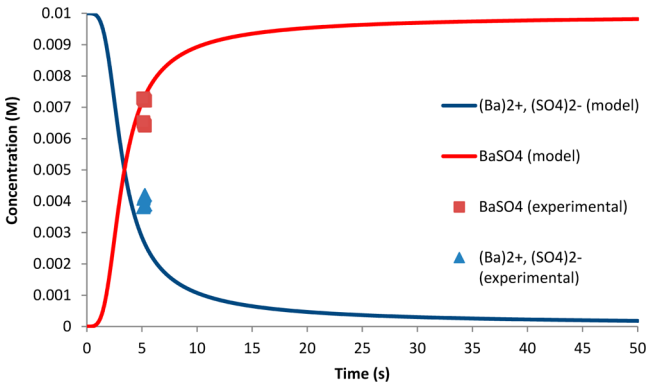


**Figure 11.** Predicted concentration vs time profiles in barium sulfate precipitation for conditions used in the present study (initial feed concentrations: 0.01 M).

of 0.4068 for feed stream concentrations of 0.01 M. Experimental concentration data, determined from measured conductivity data of the initial feed streams and of the product (with molar conductivities of $Ba^{2+}$ and $SO_4^{2-}$ at 25 °C experimentally estimated as 0.011 and 0.0092 $Sm^2/mol$, respectively, which are fairly consistent with data in the literature[47]), are also included on the plot on the basis of an extended residence time of about 5 s, the reasons for which have been discussed above. Although the experimental measurements are in reasonable agreement with the predicted concentrations, the small differences could be due to the imperfect mixing conditions downstream of the SDR causing growth to be slower in our experiments than that estimated by the model.

The concentration curves show that the reaction rate for the initial conditions ($C_{feed}$ = 0.01 M) applied here is rather slow. Thus, it takes more than 18 s to reach a 95% conversion, indicating that the comparatively shorter residence times in the SDR (of the order of 5 s if the disc and probe are considered as one entity) is a limiting factor in achieving complete conversion under the chosen experimental conditions. The maximum conversion attained in our work, corresponding to the flat portion of Figure 9, is about 65%.

The model predicts that increases in the initial feed concentrations result in drastic reduction of the reaction time constants (Table 2). Thus, for initial feed concentration of 1 M, the time required to achieve a 95% conversion is significantly reduced to 30.5 ms. The reaction times for feed concentrations of 1 M would clearly be shorter than the residence times on the disc itself. Therefore, at higher initial concentrations, it is reasonable to expect that the conversion rates would be extremely fast and, thus, independent of the overall residence times in the SDR.

From the presented analysis, it can be deduced that, for successful control of processes such as precipitations and other fast reactions in SDRs, sophisticated control algorithms may be required. Under such algorithms, the controller would be capable of taking appropriate action based on the operating window and on whether the process is controlled by residence time or mixing intensity or a combination of both.

**Table 2. Chemical Conversion Times for Various Reagent Concentrations**

| $C_{feed}$ [M] | $\gamma$ | $S$ | time at 50% conversion | time at 95% conversion |
|---|---|---|---|---|
| 0.01 | 0.4068 | 388 | 3.41 s | 18.49 s |
| 0.1 | 0.15 | 1430 | 0.2 s | 1.2 s |
| 1 | 0.0389 | 3709 | 5.4 ms | 30.5 ms |

## 5. CONCLUSIONS AND FUTURE OUTLOOK

In the present work, two example processes, namely, a neutralization reaction and a precipitation reaction, were selected to investigate the controllability of SDRs using commonly used controllers, sensors, and actuators. The pH control of a strong acid/strong base neutralization reaction was successfully achieved using a PID controller implemented in LabVIEW, coupled with commercially available instrumentation. The pH control performance exhibited the undesired effects of limit cycles near the equivalence point of pH 7 as well as sluggish response away from the neutralization point. Such behavior is expected when a linear, nonadaptive controller is applied to a highly nonlinear control problem such as that encountered in strong acid/strong base neutralization systems as studied here. The limit cycles were significantly suppressed by addition of a disturbance observer algorithm.

A PI controller implemented in LabVIEW was also shown to successfully coerce the conductivity of the effluent stream containing barium sulfate particles to the desired set point by manipulating the disc rotational speed. The presented results show that the disc rotational speed may be exploited as an extra degree of freedom in control system design. The conductivity of the effluent stream is an indication of the ion concentrations from which the degree of supersaturation may be inferred. Therefore, the particle size and morphology in a crystallization process may also be controlled by manipulating the disc rotational speed.

The experimental data on conductivity versus disc rotational speed also unveiled that a system constraint may exist, beyond which rotational speed does not influence the extent of reaction. This trend was attributed to micromixing enhancement in the lower speed range while, at the higher speeds, mixing is so fast that it no longer affects the process. Further, overall residence time in the SDR (which is dominated by the time period for the product to travel to the probe location) is shown to limit the extent of conversion reached for the concentration studied. The interactions of the film hydrodynamics on mixing and residence time highlight the need to define these effects clearly in order to achieve effective operation and control of SDRs.

The often complex relationship between the controlled variables and the manipulated variables forms the basis of devising a successful control scheme for SDRs. Depending on the complexity of the process and the interactions of the input and output parameters, advanced control schemas may be employed for control of processes in SDRs. The future developments of control strategies for SDRs would benefit from exploring more sophisticated control schemes and comparing their relative merits with those of the basic PID algorithm adopted in this study.


dx.doi.org/10.1021/ie4020149 | Ind. Eng. Chem. Res. 2013, 52, 16832−16841

It is also worth noting that the control strategies implemented here are merely passive regulatory systems, devised based on the available SDR design and the conventional sensors/actuators. Therefore, the control performance is inevitably limited by the SDR design and the performance characteristics of the available instrumentation. The measurement and transport time delays in the present control loop setup are much greater than the dynamics of the SDR and, thus, present a significant limitation on control of such devices. Therefore, intensified sensors with faster dynamics and smaller volumes may need to be developed to achieve an optimum control performance. Additionally, process control and the conceptual design of intensified equipment should ideally be considered simultaneously. There should be provisions made for embedding the new generation of sensors on the disc surface to achieve real-time measurement of the process variable within the processing films, as opposed to placing the conventional sensors downstream of the SDRs. These recommendations are rather long-term and call for the development of more elaborate sensors and equipment design. Such large leaps in instrumentation and equipment design require a lot of research endeavors and capital investments, which may put the industrial acceptance of intensified equipment on hold for a while longer.

## AUTHOR INFORMATION


### Corresponding Author

*E-mail: kamelia.boodhoo@newcastle.ac.uk. Tel:+44(0) 1912227264.

### Present Address

†M.T.T.: School of Chemical Engineering, Newcastle University Singapore, Singapore 599489.


### Notes

The authors declare no competing financial interest.

## ACKNOWLEDGMENTS

The funding for the present research was provided by an EPSRC Doctoral Training Award granted to Dena Ghiasy.

## NOMENCLATURE

$C$ [mol/dm$^3$], concentration
$D$ [m$^2$/s], diffusion coefficient
$e$ [%], error between set point and process variable
$Ek$ [−], Ekman number
$K_c$ [%/%], controller gain
$K_{sp}$ [mol$^2$/dm$^6$], solubility product
$N$ [rpm], disc speed
$Q$ [m$^3$/s], volumetric flow rate
$r$ [m], radial distance from the disc center
$S$ [−], supersaturation ratio
$Sc$ [−], Schmidt number ($\nu$/D)
$T_d$ [min], derivative time
$T_i$ [min], integral time
$t_{res}$ [s], liquid residence time on the disc
$u$ [m/s], radial velocity

### SpecialCharacters

$\gamma$ [−], activity coefficient
$\delta$ [m], film thickness
$\varepsilon$ [W/kg], energy dissipation rate
$\nu$ [m$^2$/s], kinematic viscosity
$\tau_{ind}$ [s], induction time
$\tau_{micro}$ [s], micromixing time constant
$\omega$ [rad/s], angular velocity (=2$\pi N$/60)

### Subscripts

i inlet
o outlet

## REFERENCES


(1) Ramshaw, C.; Cook, S. Spinning Around. *Chem. Engineer* **2005**, 42.
(2) Boodhoo, K. V. K. Spinning Disc Reactor for Green Processing and Synthesis. In *Process Intensification for Green Chemistry*; Boodhoo, K., Harvey, A. P., Eds.; Wiley: Chichester, 2013.
(3) Oxley, P.; Brechtelsbauer, C.; Ricard, F.; Lewis, N.; Ramshaw, C. Evaluation of Spinning Disk Reactor Technology for the Manufacture of Pharmaceuticals. *Ind. Eng. Chem. Res.* **2000**, *39*, 2175.
(4) Boodhoo, K. V. K.; Jachuck, R. J. Process Intensification: Spinning Disk Reactor for Styrene Polymerisation. *Appl. Therm. Eng.* **2000**, *20*, 1127.
(5) Boodhoo, K. V. K.; Jachuck, R. J. Process Intensification: Spinning Disc Reactor for Condensation Polymerisation. *Green Chem.* **2000**, *2*, 235.
(6) Yatmaz, H. C.; Wallis, C.; Howarth, C. R. The Spinning Disc Reactor - Studies on a Novel $TiO_2$ Photocatalytic Reactor. *Chemosphere* **2001**, *42*, 397.
(7) Vicevic, M.; Boodhoo, K. V. K.; Scott, K. Catalytic Isomerisation of Alpha-Pinene Oxide to Campholenic Aldehyde using Silica-Supported Zinc Triflate Catalysts II. Performance of Immobilised Catalysts in a Continuous Spinning Disc Reactor. *Chem. Eng. J.* **2007**, *133*, 43.
(8) Ghiasy, D.; Boodhoo, K. V. K.; Tham, M. T. Control of Intensified Equipment: A Simulation Study for pH Control in a Spinning Disc Reactor. *Chem. Eng. Process.* **2012**, *55*, 1.
(9) Lim, S. T. Hydrodynamics and Mass Transfer Processes Associated with the Absorption of Oxygen in Liquid Films Flowing Across a Rotating Disc. Ph.D. thesis, University of Newcastle upon Tyne, 1980.
(10) Aoune, A.; Ramshaw, C. Process Intensification: Heat and Mass Transfer Characteristics of Liquid Films on Rotating Discs. *Int. J. Heat Mass Transfer* **1999**, *42*, 2543.
(11) Burns, J. R.; Jachuck, R. J. Monitoring of $CaCO_3$ Production on a Spinning Disc Reactor using Conductivity Measurements. *AIChE J.* **2005**, *51*, 1497.
(12) Cafiero, L. M.; Baffi, G.; Chianese, A.; Jachuck, R. J. J. Process Intensification: Precipitation of Barium Sulfate using a Spinning Disk Reactor. *Ind. Eng. Chem. Res.* **2002**, *41*, 5240.
(13) Henson, M. A.; Seborg, D. E. Adaptive Input-Output Linearization of a pH Neutralization Process. *Int. J. Adapt. Control* **1997**, *11*, 171.
(14) Waller, K. V.; Gustafsson, T. K. Fundamental Properties of Continuous pH Control. *ISA Trans.* **1983**, *22*, 25.
(15) Shinskey, F. G. *Process Control Systems: Application, Design, and Tuning*, 4th ed.; McGraw-Hill: New York, 1996.
(16) Baldyga, J.; Podgorska, W.; Pohorecki, R. Mixing-Precipitation Model with Application to Double Feed Semibatch Precipitation. *Chem. Eng. Sci.* **1995**, *50*, 1281.
(17) Schwarzer, H. C.; Peukert, W. Combined Experimental/Numerical Study on the Precipitation of Nanoparticles. *AIChE J.* **2004**, *50*, 3234.
(18) Hu, J.; Johnston, K. P.; Williams, R. O. Nanoparticle Engineering Processes for Enhancing the Dissolution Rates of Poorly Water Soluble Drugs. *Drug Dev. Ind. Pharm.* **2004**, *30* (3), 233.
(19) Hessel, V.; Löwe, H.; Schönfeld, F. Micromixers—A Review on Passive and Active Mixing Principles. *Chem. Eng. Sci.* **2005**, *60*, 2479.
(20) McCarthy, E. D.; Dunk, W. A. E.; Boodhoo, K. V. K. Application of an Intensified Narrow Channel Reactor to the Aqueous Phase Precipitation of Barium Sulphate. *J. Colloid Interface Sci.* **2007**, *30*, 572.

(21) Boodhoo, K. V. K.; Al-Hengari, S. Micromixing Characteristics in a Small Scale Spinning Disk Reactor. *Chem. Eng. Technol.* **2012**, *35* (7), 1229.
(22) Gunn, D. J.; Murthy, M. S. Kinetics and Mechanisms of Precipitation. *Chem. Eng. Sci.* **1972**, *27*, 1293.
(23) Matynia, A.; Piotrowski, K.; Koralewska, J. Barium Sulphate Crystallization Kinetics in the Process of Barium Ions Precipitation by means of Crystalline Ammonium Sulphate Addition. *Chem. Eng. Process.* **2005**, *44*, 485.
(24) Pohorecki, R.; Baldyga, J. The Effects of Micromixing and the Manner of Reactor Feeding on Precipitaion in Stirred Tank Reactors. *Chem. Eng. Sci.* **1988**, *43*, 1949.
(25) Braatz, R. D. Advanced Control of Crystallization Processes. *Annu. Rev. Control* **2002**, *26*, 87.
(26) Alatalo, H.; Kohonen, J.; Qu, H.; Hatakka, H.; Reinikainen, S. P.; Louhi-Kultanen, M.; Kallas, J. In-line Monitoring of Reactive Crystallization Process based on ATR-FTIR and Raman Spectroscopy. *J. Chemom.* **2008**, *22*, 644.
(27) Alatalo, H.; Hatakka, H.; Kohonen, J.; Reinikainen, S. P.; Louhi-kultanen, M. Process Control and Monitoring of Reactive Crystallization of L-Glutamic Acid. *AIChE J.* **2010**, *56*, 2063.
(28) Heinrich, J.; Elter, T.; Ulrich, J. Data Preprocessing of In Situ Laser-Backscattering Measurements. *Chem. Eng. Technol.* **2011**, *34*, 977.
(29) Mersmann, A. *Crystallization Technology handbook*; Marcel Dekker: New York, 1995.
(30) Hamann, C. H.; Hamnett, A.; Vielstich, W. *Electrochemistry*; Wiley-VCH: New York, 1998.
(31) Taguchi, K.; Garside, J.; Tavare, N. S. Nucleation and Growth Kinetics of Barium Sulphate in Batch Precipitation. *J. Cryst. Growth* **1996**, *163*, 318.
(32) Stanley, S. J. Tomographic Imaging during Reactive Precipitation in a Stirred Vessel: Mixing with Chemical Reaction. *Chem. Eng. Sci.* **2006**, *61*, 7850.
(33) Rodgers, T. L.; Stephenson, D. R.; Cooke, M.; York, T. A.; Mann, R. Tomographic Imaging during Semi-Batch Reactive Precipitation of Barium Sulphate in a Stirred Vessel. *Chem. Eng. Res. Des.* **2009**, *87*, 615.
(34) Johnson, G. W.; Jennings, R. *LabVIEW Graphical Programming*, 4th ed., McGraw-Hill: New York, 2006.
(35) Seborg, D.; Edgar, T. F.; Mellichamp, D. A.; Doyle, F. J. *Process Dynamics and Control*, 3rd ed.; J.Wiley: Asia, 2011.
(36) Shahruz, S. M.; Rajarama, S. A. Suppression of Limit Cycles in a Class of Non-Linear Systems by Disturbance Observers. *J. Sound Vib.* **2000**, *229*, 1003.
(37) Shahruz, S. M.; Cloet, C.; Tomizuka, M. Suppression of Effects of Non-Linearities in a Class of Non-Linear Systems by Disturbance Observers. *J. Sound Vib.* **2002**, *249*, 405.
(38) Boodhoo, K. V. K.; Dunk, W. A. E.; Vicevic, M.; Jachuck, R. J.; Sage, V.; Macquarrie, D. J.; Clark, J. H. Classical Cationic Polymerization of Styrene in a Spinning Disc Reactor using Silica-Supported $BF_3$ Catalyst. *J. Appl. Polym. Sci.* **2006**, *101*, 8.
(39) Baldyga, J.; Bourne, J. R. *Turbulent Mixing and Chemical Reactions*; John Wiley & Sons: New York, 1999.
(40) Guo, Z.; Jones, A. G.; Li, N. The Effect of Ultrasound on the Homogeneous Nucleation of BaSO4 During Reactive Crystallization. *Chem. Eng. Sci.* **2006**, *61*, 1617.
(41) Jacobsen, N. C.; Hinrichsen, O. Micromixing Efficiency of a Spinning Disk Reactor. *Ind. Eng. Chem. Res.* **2012**, *51*, 11643.
(42) Khan, J. R. Heat transfer on a rotating surface with and without phase change. Ph.D. Thesis, University of Newcastle Upon Tyne, 1986.
(43) de Caprariis, B.; Di Rita, M.; Stoller, M.; Verdone, N.; Chianese, A. Reaction-Precipitation by a Spinning Disc Reactor: Influence of Hydrodynamics on Nanoparticle Production. *Chem. Eng. Sci.* **2012**, *76*, 73.
(44) Bromley, L. A. Thermodynamic Properties of Strong Electrolytes in Aqueous Solutions. *AIChE J.* **1973**, *19*, 313.
(45) Marchisio, D. L.; Barresi, A. A.; Garbero, M. Nucleation, Growth, and Agglomeration in Barium Sulfate Turbulent Precipitation. *AIChE J.* **2002**, *48* (9), 2039.
(46) Oncul, A. A.; Sundmacher, K.; Seidel-Morgenstern, A.; Thevenin, D. Numerical and Analytical Investigation of Barium Sulphate Crystallization. *Chem. Eng. Sci.* **2006**, *61*, 652.
(47) Laidler, K. J.; Meiser, J. H.; Sanctuary, B. C. *Physical Chemistry*, 4th ed.; Houghton Mifflin: Boston, 2002.